Stereochemical and Electronic Control of M–SO_2 Bonding Geometry in d^6 Molybdenum and Tungsten SO_2 Complexes: Novel $\eta^1 \longleftrightarrow \eta^2$ SO_2 Linkage Isomerization in $Mo(CO)_2(PPh_3)_2(CNR)(SO_2)$ and Structures of $Mo(CO)_3(P\text{-}i\text{-}Pr_3)_2(SO_2)$ and $[Mo(CO)_2(py)(PPh_3)(\mu\text{-}SO_2)]_2$

Gregory J. Kubas,* Gordon D. Jarvinen, and Robert R. Ryan

Contribution from the Los Alamos National Laboratory, University of California, Los Alamos, New Mexico 87545. *Received June 11, 1982*

Abstract: New complexes, *mer,trans*-$M(CO)_3(PR_3)_2(SO_2)$ (M = Mo, W; R = Ph, Cy, *i*-Pr) (I), *cis,trans*-$Mo(CO)_2(PPh_3)_2(SO_2)(L)$ (L = NCMe, py, CNCy, CN-*t*-Bu and CN(*p*-tolyl)) (II), and $[Mo(CO)_2(py)(PPh_3)(\mu\text{-}SO_2)]_2$, have been prepared and characterized by infrared spectroscopy, ^{17}O and ^{31}P NMR spectroscopy, and X-ray crystallography. Syntheses for *fac*-$Mo(CO)_3(\eta^2\text{-}SO_2)(LL)$ (LL = dppe, bpy, phen, 2 py) have also been developed. Depending upon L, II has been found to coordinate SO_2 either in the S-bonded (η^1 planar) or O,S-bonded (η^2) geometries. Remarkably, for L = CNCy or CN-*t*-Bu, II has been found to contain, in the solid state, an apparent equimixture of *both* coordination types. Isomerization of *fac*-$M(CO)_3(dppe)(\eta^2\text{-}SO_2)$ (M = Mo, W; dppe = 1,2-bis(diphenylphosphino)ethane) to an η^1-planar SO_2 form, *mer*-$M(CO)_3(dppe)(SO_2)$, has also been found to occur. Thus, control of the SO_2 coordination geometry has been achieved by varying either the electronic properties of the ancillary ligands or their disposition with respect to the SO_2. The X-ray crystal structure of *mer,trans*-$Mo(CO)_3(P\text{-}i\text{-}Pr_3)_2(SO_2)$ revealed η^1-planar SO_2 binding, the first example of this geometry for group 6 metals. The M–S distance, 2.239 (3) Å, is the longest such distance for this geometry recorded to date. Crystal data: *Pbca*, Z = 8, a = 24.712 (8) Å, b = 16.033 (6) Å, c = 14.058 (5) Å, R = 0.079 for 2934 reflections with $I \geq 2\sigma(I)$. The structure of $[Mo(CO)_2(py)(PPh_3)(\mu\text{-}SO_2)]_2$ showed a novel SO_2 bridging geometry in which all three atoms of SO_2 are metal coordinated. Crystal data: $P\bar{1}$, Z = 1, a = 14.833 (4) Å, b = 9.264 (2) Å, c = 10.808 (2) Å, R = 0.039 for 3282 reflections with $I \geq 2\sigma(I)$.

We have been investigating the chemistry of zerovalent molybdenum and tungsten sulfur dioxide complexes upon recently discovering that side-on (η^2) bonding of SO_2 occurs in these systems.[1,2] This bonding mode has been of considerable interest in terms of S–O bond activation, as exemplified by the novel reactivity of the coordinated SO_2 in $Ru(CO)_2(PPh_3)_2(\eta^2\text{-}SO_2\cdot SO_2)$.[3] Furthermore, group 6 complexes of SO_2 had been relatively unexplored, and examples of η^1-planar SO_2 coordination, the predominant mode for d^6 complexes in general, were unknown. This work describes the synthesis and characterization of η^1-planar complexes as well as new η^2-SO_2 complexes. More significantly, control of the SO_2 bonding mode has been achieved by proper choice of the σ-donating vs. π-accepting ancillary ligands as well as their geometric disposition with respect to the SO_2. For example, the SO_2 ligand in *cis,trans*-$Mo(CO)_2(PPh_3)_2(SO_2)(L)$ has been found to coordinate in either η^1-planar or η^2 fashion, depending upon the nature of L. Moreover, a unique situation was encountered for the complex containing L = alkylisocyanide: *the coexistence of both an η^1-planar SO_2 isomer and an η^2-SO_2 isomer in apparent equimixture.* This is the first example of spontaneous linkage isomerism of coordinated SO_2. In addition to electronic effects, the steric arrangement of the ancillary ligands also influences the SO_2 bonding mode, as will be shown below.

The first structurally characterized example of coordination of all three atoms of SO_2 to metal atoms was recently reported for the complex $[Mo(CO)_2(py)(PPh_3)(\mu\text{-}SO_2)]_2$.[4] Further detail concerning synthesis, characterization, and reactions of this dimer is presented here.

Experimental Section

All preparations were carried out in a nitrogen or SO_2 atmosphere, and products were generally collected on a frit, washed with an appropriate solvent, and dried briefly in vacuo. Phosphines and metal carbonyls were purchased from Strem Chemicals, Newburyport, MA, and CN-*t*-Bu and CNC_6H_{11} from Tridom Chemical, Hauppauge, NY; $M(CO)_3(NCMe)_3$,[5] $W(CO)_3(C_7H_8)$ (C_7H_8 = η^6-cycloheptatriene),[6] *cis,trans*-$Mo(CO)_2(PPh_3)_2(NCMe)_2$,[7] and *p*-tolylisocyanide[8] were prepared by published procedures. Infrared spectra were recorded on a Perkin-Elmer 521, and elemental analyses were performed by Galbraith Laboratories, Knoxville, TN.

Preparation of *mer,trans*-$Mo(CO)_3(P\text{-}i\text{-}Pr_3)_2(SO_2)$ (Ia). To a solution of $Mo(CO)_3(C_7H_8)$ (0.544 g, 2 mmol) in 5 mL of benzene was added $P\text{-}i\text{-}Pr_3$ (0.79 mL, 4 mmol). The reaction mixture was stirred for 30 min, treated with excess SO_2, and allowed to stir another 15 min. Addition of heptane (15 mL) and cooling for 6 h in a freezer gave a solid, which was collected, washed with a small amount of heptane, and extracted with ether (10 mL). The filtered solution was reduced in volume to ca. 2 mL, treated with 3 mL of heptane, and reduced again to 2 mL in vacuo. The yield of heptane-washed red microcrystals of Ia was 0.23 g (20%).

Ia can also be prepared in a similar manner from $Mo(CO)_3(NCMe)_3$, but oily, impure products often result. Ia is relatively air-stable in the solid state but should be stored in a freezer or in an inert atmosphere, since long-term exposure to air and light produced partial decomposition. Ia is quite soluble even in nonpolar solvents, and solutions exposed to air yielded dark colored precipitates, infrared spectra of which showed weak carbonyl bands but no bands ascribable to bidentate sulfate.

Preparation of *mer,trans*-$Mo(CO)_3(PCy_3)_2(SO_2)$ (Ib). $Mo(CO)_3(C_7H_8)$ (0.467 g) and PCy_3 (0.97 g) were stirred overnight in 5 mL of toluene saturated with SO_2. Methanol (10 mL) was added to the reaction mixture to complete precipitation of the product, the yield of which after washing with methanol was 0.56 g (40%).

Preparation of *mer,trans*-$W(CO)_3(P\text{-}i\text{-}Pr_3)_2(SO_2)$ (Ic). Method A. A slurry of $W(CO)_3(NCMe)_3$ (0.440 g, 1.13 mmol) in 5 mL of acetone was treated with $P\text{-}i\text{-}Pr_3$ (0.46 mL). Most of the solids dissolved within 5–10 min, whereupon a light yellow precipitate then formed rapidly. After the mixture was stirred another 10 min, excess SO_2 was added, giving a red solution and a small amount of red solid. The solvent was removed in vacuo, and the resulting residue was extracted with ether (10

(1) Kubas, G. J.; Ryan, R. R.; McCarty, V. *Inorg. Chem.* **1980**, *19*, 3003.
(2) Ryan, R. R.; Kubas, G. J.; Moody, D. C.; Eller, P. G. *Struct. Bonding (Berlin)* **1981** *46*, 47.
(3) Moody, D. C.; Ryan, R. R. *J. Chem. Soc., Chem. Commun.* **1980**, 1230.
(4) Jarvinen, G. D.; Kubas, G. J.; Ryan, R. R. *J. Chem. Soc., Chem. Commun.* **1981**, 305.
(5) Tate, D. P.; Knipple, W. R.; Augl, J. M. *Inorg. Chem.* **1962**, *1*, 433.
(6) King, R. B.; Fronzaglia, A. *Inorg. Chem.* **1966**, *5*, 1837; the use of $W(CO)_3(NCEt)_3$ (ref 9) and heptane as starting material and solvent was found to improve the yield of large-scale reactions (49% for a 74-mmol scale).
(7) tom Dieck, H.; Friedel, H. *J. Chem. Soc. D* **1969**, 411.
(8) Weber, W. P.; Gokel, G. W.; Ugi, I. K. *Angew. Chem., Int. Ed. Engl.* **1972**, *11*, 530.

0002-7863/83/1505-1883$01.50/0

mL). Reduction of the volume of the filtered extract to 2–3 mL followed by addition of heptane (4 mL) gave (Ic), which was washed with heptane and weighed 0.40 g (54%). The product, despite showing a clean IR spectrum, was slightly oily and off-color, but recrystallization readily afforded a pure, red-brown product. Ic is somewhat less soluble and more stable than Ia.

Method B. A solution of $W(CO)_3(C_7H_8)$ (0.182 g, 0.506 mmol) in 3 mL of ether was treated with P-*i*-Pr_3 (0.21 mL) and stirred for 15 min. SO_2 addition followed by heptane (5 mL) addition and reduction of solvent volume to 5 mL gave Ic (0.170 g, 52%), which was isolated as above.

Preparation of *mer,trans*-$W(CO)_3(PCy_3)_2(SO_2)$ (Id). Method A. A slurry of $W(CO)_3(NCEt)_3$[9] (3.24 g) and PCy_3 (4.30 g) in 40 mL of acetone was stirred for ca. 10 min. A light yellow voluminous precipitate formed, and stirring was continued for 10 min. Saturation of the reaction mixture with SO_2 followed by heptane (5 mL) addition gave Id (5.44 g, 81%), isolated as above. The use of $W(CO)_3(NCMe)_3$ resulted in lower yields (50%).[9]

Method B. $W(CO)_3(C_7H_8)$ (0.18 g), PCy_3 (0.28 g), and toluene (2 mL) were stirred for ca. 25 min, resulting in formation of a yellow precipitate of $W(CO)_3(PCy_3)_2(N_2)$.[10] Upon SO_2 addition, slow displacement of coordinated N_2 occurred. The reaction mixture was stirred for 1 h in an SO_2 atmosphere during which time Id precipitated. Addition of heptane (5 mL) gave an 80% yield (0.355 g) of Id.

Preparation of *mer,trans*-$Mo(CO)_3(PPh_3)_2(SO_2)$ (Ie). A slurry of *cis,trans*-$Mo(CO)_2(PPh_3)_2(SO_2)$(NCMe) (0.179 g) in 5 mL of benzene was treated with excess CO. Within several minutes a bright deep red solution formed, whereupon excess SO_2 was immediately added in place of the CO. Precipitation of product soon began and was completed by addition of SO_2-saturated heptane (10 mL); yield, 0.150 g (85%).

Ie is an air-stable solid but is unstable in solution toward isomerization or compositional changes even in an inert atmosphere.

Preparation of *cis,trans*-$Mo(CO)_2(PPh_3)_2(SO_2)$(NCMe) (II, L = NCMe). A rapid stream of SO_2 was passed over a magnetically stirred slurry of *cis,trans*-$Mo(CO)_2(PPh_3)_2(NCMe)_2$ (5.25 g) in 70 mL of MeCN. The reaction mixture became very warm, and violet microcrystals of II (L = NCMe) began to form within minutes. Stirring was continued for 15 min while maintaining an SO_2 atmosphere in the reaction flask, which was then placed into the freezer compartment of a refrigerator overnight to complete precipitation of the product. The yield of MeCN-washed crystals was 4.51 g (83%). II (L = NCMe) is moderately air-sensitive in the solid state and sparingly soluble in MeCN. Disproportionation and/or isomerization occurs in CH_2Cl_2 solution.

Preparation of *cis,trans*-$Mo(CO)_2(PPh_3)_2(SO_2)$(CNR) (II, L = CNR). A stoichiometric amount of RNC was added to a stirred solution of II (L = NCMe) (0.55 g, 0.7 mmol) in CH_2Cl_2 (4 mL). The solution soon began to deposit a crystalline precipitate of II (L = CNR), and stirring was continued for 10 min, whereupon 20 mL of diethyl ether was slowly added from a dropping funnel to complete precipitation. The yield of ether-washed product was 83% (ca. 0.5 g).

The complexes are air-stable solids that when viewed through transmitted light appear orange-brown but when finely ground in a mortar are olive green in color. CH_2Cl_2 solutions of II (L = alkylisocyanide) are relatively stable in an inert atmosphere.

Preparation of *cis,trans*-$Mo(CO)_2(PPh_3)_2(SO_2)$(py) (II, L = py). A slurry of II (L = NCMe) (0.228 g) in 4 mL of methanol was treated with 0.048 mL of pyridine and stirred vigorously for 6 min. The resulting air-stable solid was washed with ether and weighed 0.193 g (81%). The complex is unstable in solution and also slowly decomposes in the solid state over an extended period.

Isomerization of $Mo(CO)_2(PPh_3)_2(SO_2)$(py). A solution of II (L = py) (0.4 g, 0.49 mmol) and PPh_3 (0.6 g, 2.3 mmol; to suppress dimer formation) in 2 mL of CH_2Cl_2 was stirred for exactly 4 min and immediately treated with 12 mL of ether. The dark lavender precipitate (~0.21 g) was filtered off, washed with ether, and dried. The yield and purity of the product depended upon reaction conditions (especially time), and ~10% of the product consisted of II (L = py) and/or $[Mo(CO)_2(PPh_3)(py)(\mu\text{-}SO_2)]_2$.

Similar results were obtained if II (L = py) was generated in situ from II (L = NCMe) and a slight stoichiometric excess of pyridine in the presence of excess PPh_3. The isomer gave elemental analyses (Table I) (supplementary material) nearly identical with II (L = py) but displayed different infrared frequencies.

Preparation of $[Mo(CO)_2(py)(PPh_3)(\mu\text{-}SO_2)]_2 \cdot 2CH_2Cl_2$. II (L = NCMe) (0.717 g, 0.917 mmol) was dissolved in 5 mL of CH_2Cl_2 and immediately treated with 0.1 mL (1.24 mmol) of pyridine. The reaction mixture was allowed to stand overnight, and the resulting crystalline precipitate was washed with 20 mL of 1:1 ether–CH_2Cl_2 and dried in a nitrogen stream (yield, 0.38 g, 70%). Additional product (0.08 g) was obtained on allowing the filtrate to stand further.

The dimer was also found to crystallize even if a large excess of pyridine was used (ether addition was necessary) and can also be prepared by allowing a solution of II (L = py) in CH_2Cl_2 to stand with no added pyridine. It readily loses lattice CH_2Cl_2 in vacuo or upon washing with non CH_2Cl_2 containing solvents.

Preparation of $[Mo(CO)_2(CyNH_2)(PPh_3)(\mu\text{-}SO_2)]_2$. II (L = NCMe) (0.276 g, 0.353 mmol) in 5 mL of CH_2Cl_2 was treated with 0.065 mL (0.54 mmol) of cyclohexylamine. After 15 min, the volume of the solution was reduced to ca. 2 mL, and a dark brown microcrystalline precipitate formed. The reaction mixture was allowed to stand for 10 min, and diethyl ether (5 mL) was then added slowly to complete the precipitation. After another 10 min, the precipitate was washed with 1:1 ether–CH_2Cl_2; the yield was 0.175 g (86%). In some instances a small amount of fine pink insoluble precipitate formed prior to crystallization of $[Mo(CO)_2(CyNH_2)(PPh_3)(\mu\text{-}SO_2)]_2$. This material was identified to be $Mo(CO)_2(CyNH_2)_3(SO_2)$ by X-ray crystallography[11] and can be removed by filtration.

Preparation of $[Mo(CO)_2(py)_2(\mu\text{-}SO_2)]_2$. A mixture containing 0.15 g (0.12 mmol) of $[Mo(CO)_2(PPh_3)(py)(\mu\text{-}SO_2)]_2$ and 3 mL of 3:1 CH_2Cl_2–pyridine was stirred overnight, and the resulting poorly soluble precipitate (0.03 g, 32%) was isolated as above.

Reaction of $[Mo(CO)_2(py)(Ph_3)(\mu\text{-}SO_2)]_2$ with Excess $P(OMe)_3$; Formation of $Mo(CO)_2[P(OMe)_3]_3(SO_2)$. The dimer (100 mg), CH_2Cl_2 (3 mL), and $P(OMe)_3$ (1 mL) were stirred overnight. Partial solvent removal and addition of excess heptane yielded 40 mg of a complex that was formulated to be $Mo(CO)_2[P(OMe)_3]_3(SO_2)$ on the basis of elemental analysis (Table I) and infrared spectroscopy (Table II) (supplementary material).

Reaction of II (L = NCMe) with Bipyridyl To Form $Mo(CO)_2(bpy)(PPh_3)_2$. Bipyridyl (0.05 g, 0.32 mmol) was added to a solution of II (L = NCMe) (0.24 g, 0.31 mmol) in 5 mL of CH_2Cl_2, resulting in the immediate formation of a deep green precipitate. The latter was identified to be $Mo(CO)_2(bpy)(PPh_3)_2$ by comparison of its properties with those reported in the literature;[12] yield, 0.22 g (85%).

Preparation of *cis,trans*-$Mo(CO)_2(PPh_3)_2(CNR)_2$ (R = Cy, *t*-Bu, or *p*-Tolyl). The appropriate isocyanide (1.0 mmol) was added to a stirred slurry of $Mo(CO)_2(PPh_3)_2(NCMe)_2$ (0.38 g, 0.5 mmol) in CH_2Cl_2 (2 mL), resulting in formation of a yellow solution. Addition of 10 mL of ether gave yellow microcrystals, which were washed with ether. Yields of $Mo(CO)_2(PPh_3)_2(CNR)_2$ ranged from 80–89%.

Preparation of *fac*-$M(CO)_3(dppe)(\eta^2\text{-}SO_2)$. A solution of $Mo(CO)_3(NCMe)_3$ (1.57 g, 5.18 mmol) and dppe (2.03 g, 5.11 mmol) in 250 mL of acetonitrile was heated to reflux for 20 h. The warm solution was filtered and refrigerated overnight. A crop of pale yellow crystals of *fac*-$Mo(CO)_3(dppe)(NCMe)$ was isolated (1.65 g, 52%) with $\nu(CO)$ (1933 s, 1840 s, 1819 s cm^{-1} in CH_2Cl_2) in good agreement with the values reported by Dobson and Houk.[13] In 15 mL of CH_2Cl_2 saturated with SO_2, 0.515 g of $Mo(CO)_3(dppe)(NCMe)$ was dissolved to give a deep red solution. After 30 min, 30 mL of MeOH was added and the solution cooled to −20 °C in a freezer. After several hours, dark red crystals of *fac*-$Mo(CO)_3(dppe)(\eta^2\text{-}SO_2)$ were isolated (0.169 g, 32%).

In the presence of a large excess of MeCN at room temperature in CH_2Cl_2, the η^2-SO_2 complex converts back to *fac*-$Mo(CO)_3(dppe)$-(NCMe) in about 2 h.

Isomerization of *fac*-$Mo(CO)_3(dppe)(\eta^2\text{-}SO_2)$ to *mer*-$Mo(CO)_3(dppe)(\eta^1\text{-}SO_2)$. Solutions of *fac*-$Mo(CO)_3(dppe)(\eta^2\text{-}SO_2)$ were found to slowly isomerize to the *mer* isomer at room temperature. Monitoring of the $\nu(CO)$ bands as the isomerization proceeded gave a $t_{1/2}$ of about 8 h at 20 °C in CH_2Cl_2. In one experiment, 0.248 g of *fac*-$Mo(CO)_3(dppe)(\eta^2\text{-}SO_2)$ was dissolved in 50 mL of CH_2Cl_2. The red solution gradually became yellow. After 48 h, the CH_2Cl_2 was removed at reduced pressure and the residue dissolved in 20 mL of 5:1 acetone–heptane. The solution was filtered and the volume reduced to about 8 mL by gentle heating under a slow nitrogen flow. Cooling to 20 °C overnight gave 0.093 g of orange crystals of *mer*-$Mo(CO)_3(dppe)(\eta^1\text{-}SO_2)$.

Attempts to add a proton or BF_3 to the terminal oxygen of the η^2-SO_2 ligand in *fac*-$Mo(CO)_3(dppe)(\eta^2\text{-}SO_2)$ led to rapid isomerization to the

(9) Kubas, G. J. *Inorg. Chem.*, in press. Prepared in a manner similar to that in ref 5, except that propionitrile was used instead of acetonitrile. The solubility of $W(CO)_3(NCEt)_3$ was found to be considerably greater than that of the NCMe analogue, and substitution reactions generally proceeded much more cleanly and rapidly. Also, the reaction of $W(CO)_6$ (35 g) with NCEt (300 mL) was complete in 6 days whereas up to 2 weeks were required for the $W(CO)_3(NCMe)_3$ preparation (at an elevation of 7100 ft).

(10) Kubas, G. J. *J. Chem. Soc., Chem. Commun.* **1980**, 61.

(11) Kubas, G. J.; Ryan, R. R., manuscript in preparation.

(12) Hull, C. G.; Stiddard, M. H. B. *J. Chem. Soc. A* **1968**, 710.

(13) Dobson, R.; Houk, L. W. *Inorg. Chim. Acta* **1967**, *1*(2), 287.

mer η^1-SO_2 complex. Addition of an equimolar amount of HCl or BF_3 gas above a stirring CH_2Cl_2 solution of the *fac* complex or stirring the CH_2Cl_2 solution with excess HBF_4 resulted in a color change from red to yellow in a few minutes. The IR spectra indicated almost complete conversion to the *mer* complex in 30 min.

Photochemical Preparation of *mer*-Mo(CO)$_3$(dppe)(η^1-SO_2). A literature method was used to prepare $Mo(CO)_4$(dppe);[14] $Mo(CO)_4$(dppe) (269 mg) was dissolved in 30 mL of benzene saturated with SO_2. The water-cooled flask was irradiated with a 550-W Hanovia medium-pressure mercury arc lamp (filtered by the Pyrex glassware). The initially pale yellow solution gradually became a clear red. After 2 h of irradiation the ν(CO) bands of the starting complex were nearly gone. The benzene was removed at reduced pressure and the residue crystallized from 5:1 acetone–heptane as reported above to give 0.075 g (26%) of *mer*-$Mo(CO)_3$(dppe)(η^1-SO_2).

Isomerization of *fac*-W(CO)$_3$(dppe)(η^2-SO_2) and Preparation of *mer*-W(CO)$_3$(dppe)(η^1-SO_2). The complex *fac*-$W(CO)_3$(dppe)(NCMe) was prepared by a route very similar to the Mo analogue. However, a Soxhlet extraction with acetonitrile of the less soluble material from the reaction of $W(CO)_3(NCMe)_3$ and dppe was used to obtain the final microcrystalline product.

The displacement of acetonitrile from the W complex by SO_2 took place much less rapidly than in the Mo case. In fact, the isomerization to the *mer* η^1-SO_2 complex proceeded at a rate comparable to the formation of the *fac* η^2-SO_2 complex, and we were unable to obtain the *fac* complex free of the *mer* isomer. The progress of the reaction could be readily monitored by IR, and the ν(CO) and ν(SO) bands of the *fac* and *mer* complexes are reported in Table II. In a typical reaction, 0.266 g of $W(CO)_3$(dppe)(NCMe) was dissolved in 30 mL of acetone saturated with SO_2. After 24 h at room temperature, about 30 mL of heptane was added slowly until a slight cloudiness began to appear. The solution was cooled to 0 °C for several hours, and a crop of orange crystals (0.133 g, 48%) of *mer*-$W(CO)_3$(dppe)(η^1-SO_2) was collected.

Improved Preparations of *fac*-Mo(CO)$_3$(bpy)(η^2-SO_2) and *fac*-Mo(CO)$_3$(phen)(η^2-SO_2). A solution of $Mo(CO)_6$ (2.64 g) in 75 mL of MeCN was refluxed overnight, cooled to ca. 40 °C, and treated with bpy (1.56 g) to produce an immediate color change from yellow to deep red. The solution was filtered (if necessary) and saturated with a slow stream of SO_2. Deep purple microcrystals of $Mo(CO)_3$(bpy)(η^2-SO_2) began to form, and the reaction mixture was allowed to cool to room temperature with stirring. The product (3.645 g, 91%, based on $Mo(CO)_6$) was then collected and washed with ether.

The above scheme can presumably also be used to prepare Mo(CO)$_3$(phen)(η^2-SO_2) and other analogues, including the tungsten species, although this was not checked. The phen complex was synthesized by refluxing $Mo(CO)_4$(phen) (1.1 g) in 50 mL of MeCN for 2 h, isolating the resulting precipitate, redissolving it in 250 mL of MeCN (equivalent results can probably be obtained by adding 200 mL of MeCN without intermediate isolation), and passing SO_2 into the solution. The yield of microcrystalline $Mo(CO)_3$(phen)(η^2-SO_2) was 0.7 g.

Improved Preparation of *fac*-M(CO)$_3$(py)$_2$(η^2-SO_2) (M = Mo, W). A slurry of $M(CO)_3(NCMe)_3$ (0.533 g) in 5 mL of CH_2Cl_2 was treated with pyridine (0.29 mL), resulting in formation of an orange-red solution after several minutes. Passage of excess SO_2 into the latter yielded a deep red solution, and subsequent addition of heptane (10 mL) gave an oil, which rapidly crystallized upon stirring. The resulting red-brown solid was washed with ether and weighed 0.58 g (82%).

Preparation of the tungsten species was analogous except that a sparingly soluble yellow-brown impurity formed after SO_2 addition. However, the latter was readily removed by recrystallization from CH_2Cl_2–heptane.

Reactions of Mo–SO_2 Complexes with $MeSO_3F$ and Lewis Acids. A solution of 0.57 g of $W(CO)_3(py)_2(\eta^2\text{-}SO_2)$ in 5 mL of CH_2Cl_2 was treated with 0.2 mL of $MeSO_3F$. After 2 h a dark red oil formed that could not be induced to crystallize, and the reaction mixture gave off a persistent stench unquestionably due to organosulfur(II) species. Similar intractable products resulted for reactions of $MeSO_3F$ with $Mo(CO)_3(py)_2(\eta^2\text{-}SO_2)$ and $[Mo(CO)_2(py)(PPh_3)(\mu\text{-}SO_2)]_2$. The η^1-planar SO_2 complex, $W(CO)_3(PCy_3)_2(SO_2)$, was unreactive in toluene, as was a CH_2Cl_2 slurry of the sparingly soluble $Mo(CO)_3$(bpy)(η^2-SO_2).

A solution of 0.2 g of $Mo(CO)_3(py)_2(\eta^2\text{-}SO_2)$ in 3 mL of CH_2Cl_2 (dried over P_2O_5) was treated with 3 equiv of BF_3 on a vacuum line at −196 °C. Upon warming to −45 °C, the solution became browner in color, and removal of volatiles at 45 °C gave a brown sticky solid soluble in polar solvents. Recrystallization from CH_3CN–ether yielded an oil that crystallized upon repeated washing with ether. The infrared spectrum of the latter showed a strong broad peak at ~1050 cm^{-1} characteristic of BF_4^-. The volatiles removed from the reaction mixture contained no unreacted BF_3, also indicating that decomposition rather than simple 1:1 addition of BF_3 to coordinated SO_2 occurred. Similar experiments using Et_3Al or copper(II) hexafluoroacetylacetonate as Lewis acid also failed to yield adducts.

Table III. Crystal Data

complex	Ia	II (*L* = CNCy)	III
space group	*Pbca*	$P2_1/a$	$P\bar{1}$
a, Å	24.712 (8)	23.52 (1)	14.833 (4)
b, Å	16.033 (6)	19.58 (1)	9.264 (2)
c, Å	14.058 (5)	10.316 (5)	10.808 (2)
α, deg			93.13 (2)
β, deg		120.82 (3)	98.23 (2)
γ, deg			110.54 (2)
z	8	4	1
μ(Mo Kα), cm^{-1}	6.8		7.3
faces	{010}, {111}		{100}, {010}, {001}
d from origin, mm	0.08, 0.15		0.04, 0.12, 0.18
transmission[15]	0.92–0.82		0.95–0.84
$2\theta \geq$ deg	45		45
no. unique reflections	3540		3593
no. $\geq 2\sigma(I)$	2934		3282
unweighted *R* value, %	7.9		3.9
collection method	θ–2θ (1.5° + disp)		θ–2θ (1.5 + disp)
background, s	20		20
diffractometer	Picker FACS-1, P. G. Lenhert's Disk Operating System,[16] Wang encoders, graphite monochromator, 3.5° take-off angle, Mo Kα radiation (γ 0.709 30 Å).		

Preparation of ^{17}O-Labeled Compounds. An isotopic mixture of SO_2 species containing 33% ^{17}O and 67% ^{18}O, prepared by the reaction of S_8 with labeled NO, was kindly supplied by Dr. David Moody of our group. The labeled complexes, II (L = CNR) and *fac*-$Mo(CO)_3(py)_2(\eta^2\text{-}SO_2)$, were prepared as herein reported except that the labeled SO_2 was added in slight stoichiometric excess to the appropriate starting material by using vacuum line techniques.

^{17}O and ^{31}P NMR. ^{17}O NMR experiments were performed by Dr. Lee J. Todd of Indiana University on the aforementioned labeled complexes. Spectra were obtained with a Varian XL-100-15 spectrometer operating in the pulsed Fourier transform mode at 13.57 MHz. A pulse width of 20 μs followed by a pulse interval of 0.11 s was used for each scan. An average of 8K transients were obtained for each enriched sample. A spectral width of 10 000 Hz was used. The NMR tubes were loaded in a dry box with CH_2Cl_2 as a solvent. They were then frozen in liquid N_2, evacuated, and sealed off.

^{31}P NMR spectra were obtained from the Colorado State University Regional NMR Center. The spectra were recorded on a Nicolet NT-150 instrument.

X-ray Diffraction Measurements and Structure Solution. Single-crystal X-ray data has been obtained for three new complexes in the series, i.e., $[Mo(CO)_2(py)(PPh_3)(\mu\text{-}SO_2)]_2$ (III), $Mo(CO)_3(P\text{-}i\text{-}Pr_3)_2(SO_2)$ (Ia), and $Mo(CO)_2(PPh_3)_2(SO_2)$L (II (L = CNCy)). Pertinent information concerning the unit cells, crystal morphology, intensity measurements, etc., is given in Table III. Although we examined crystals from several samples of II (L = CNCy) crystallized under different conditions, we were unable to find a crystal suitable for accurate intensity measurements; all of them showed severe splitting. Therefore only the unit cell is reported here.

Intensities were collected for complexes Ia and III as indicated in Table III. For each of these, two standard reflections were measured after every 50 intensity measurements and indicated no crystal decomposition. The variance for F^2 (denotes the average of F^2 over equivalent reflections) was computed from $\sigma^2(\overline{F^2}) = \sigma_c^2(\overline{F^2}) + \sigma_N^2(\overline{F^2})^2$ where σ_c^2 is the variance due to counting statistics and σ_N is taken to 0.015. The function minimized in the least-squares refinements was $\sum w(|F_o| - |F_c^*|)^2$ where $w = 4F_o^2/\sigma(\overline{F^2})^2$ and F^* includes a correction for secondary extinction. Both structures were solved by standard Patterson and difference Fourier methods. Refinements were carried out by using suitable

(14) Zingales, F.; Canziani, F. *Gazz. Chim. Ital.* **1962**, *92*, 343.
(15) (a) deMeulenaer, J.; Tompa, H. *Acta Crystallogr.* **1964**, *19*, 1014. (b) Templeton, L. K.; Templeton, D. H. "Abstracts of Papers", American Crystallographic Association Summer Meeting, Storrs, CT, June 1973, No. E10.
(16) Lenhert, P. G. *J. Appl. Crystallogr.* **1975**, *8*, 568.
(17) (a) Zachariasen, W. H. *Acta Crystallogr.* **1967**, *23*, 558. (b) Larson, A. C. *Ibid.* **1967**, *23*, 664.

Table IV. Selected Distances (Å) and Angles (deg) for $Mo(CO)_3(P\text{-}i\text{-}Pr_3)_2(SO_2)$

Mo-C(1)	2.02 (1)	S-O(4)	1.46 (1)
Mo-C(2)	2.02 (1)	S-O(5)	1.48 (1)
Mo-C(3)	2.04 (1)	C(1)-O(1)	1.11 (1)
Mo-S	2.285 (3)	C(2)-O(2)	1.13 (1)
Mo-P(1)	2.544 (3)	C(3)-O(3)	1.09 (1)
Mo-P(2)	2.551 (3)		
S-Mo-C(1)	85.4 (4)	C(1)-Mo-P(2)	94.0 (4)
S-Mo-C(2)	90.6 (3)	C(2)-Mo-C(3)	94.4 (4)
S-Mo-C(3)	174.2 (3)	C(2)-Mo-P(1)	87.6 (3)
S-Mo-P(1)	96.6 (1)	C(2)-Mo-P(2)	90.0 (3)
S-Mo-P(2)	90.8 (1)	C(3)-Mo-P(1)	86.5 (3)
C(1)-Mo-C(2)	174.3 (4)	C(3)-Mo-P(2)	86.2 (3)
C(1)-Mo-C(3)	89.8 (5)	P(1)-Mo-P(2)	172.1 (1)
C(1)-Mo-P(1)	89.0 (3)	O(4)-S-O(5)	116.8 (6)

Table V. Selected Distances (Å) and Angles (deg) for $[Mo(CO)_2(PPh_3)(Py)(\mu\text{-}SO_2)]_2$

Mo-C(1)	1.889 (6)	C(1)-O(1)	1.178 (6)
Mo-C(2)	1.991 (7)	C(2)-O(2)	1.156 (7)
Mo-S	2.419 (2)	S-O(3)	1.521 (4)
Mo-O(3)	2.188 (4)	S-O(4)	1.498 (4)
Mo-O(4)	2.243 (3)		
Mo-N	2.283 (4)		
Mo-P	2.531 (2)		
C(1)-Mo-C(2)	87.6 (2)	O(3)-Mo-S	38.1 (1)
C(1)-Mo-O(3)	93.8 (2)	O(3)-Mo-O(4)	83.2 (1)
C(1)-Mo-S	88.7 (2)	O(3)-Mo-N	77.7 (1)
C(1)-Mo-O(4)	171.7 (2)	O(3)-Mo-P	167.6 (1)
C(1)-Mo-N	90.6 (2)	S-Mo-O(4)	93.5 (1)
C(1)-Mo-P	93.5 (2)	S-Mo-N	115.6 (1)
C(2)-Mo-O(3)	111.5 (2)	S-Mo-P	152.2 (1)
C(2)-Mo-S	73.6 (2)	O(4)-Mo-N	81.3 (1)
C(2)-Mo-O(4)	100.7 (2)	O(4)-Mo-P	88.2 (1)
C(2)-Mo-N	170.6 (2)	N-Mo-P	92.2 (1)
C(2)-Mo-P	78.8 (2)	O(3)-S-O(4)	111.7 (2)

neutral atom scattering factors and appropriate values for the dispersion terms.[18] Anisotropic thermal parameters were refined for all atoms heavier than hydrogen. Hydrogen atoms were located and refined (B fixed at 5.0) for complex III but were not located for complex Ia. For complex III the dimer contains a crystallographically imposed inversion center.

Distances and angles are presented for Ia and III in Tables IV and V, respectively, corresponding to the lettering scheme given in Figures 1 and 2. Atomic coordinates are given in Tables VIII and IX (supplementary material) and Tables X and XI.

Results

Preparation and Properties of $M(CO)_3L_2(SO_2)$-Type Complexes. Complexes of the type *fac*-$Mo(CO)_3L_2(\eta^2\text{-}SO_2)$ (L_2 = bpy, phen, or 2(py)), were originally synthesized by Hull and Stiddard[12] and were later found to contain η^2-SO_2 (Figures 3 and 4).[1] In the course of devising improved syntheses for these complexes, it was discovered that SO_2 readily replaces coordinated MeCN in Mo(O) complexes, even in MeCN solution (eq 1). The

$$Mo(CO)_6 \xrightarrow[\text{reflux}]{\text{MeCN}} fac\text{-}Mo(CO)_3(NCMe)_3 \xrightarrow[-2\text{NCMe}]{\text{bpy}} fac\text{-}Mo(CO)_3(bpy)(NCMe) \xrightarrow[-\text{NCMe}]{SO_2\ (\text{excess})} fac\text{-}Mo(CO)_3(bipy)(\eta^2\text{-}SO_2) \quad (1)$$

syntheses can be carried out in one vessel and give excellent yields. Although the SO_2 cannot be reversibly removed from the solid complex,[19] the SO_2 is displaceable in solution, and the final step in eq 1 can be reversed by briefly refluxing $Mo(CO)_3(bpy)(\eta^2\text{-}SO_2)$ in MeCN. In order to test the effect of ancillary ligand changes on M–SO_2 coordination geometry, preparations analogous to eq 1 using phosphines instead of nitrogen donors were tried. Use of the bidentate phosphine, dppe, led to isolation of *fac*-$Mo(CO)_3(dppe)(\eta^2\text{-}SO_2)$ with ν(SO) and ν(CO) frequencies quite similar to the previously known bpy and phen complexes. The *fac*-$Mo(CO)_3(dppe)(\eta^2\text{-}SO_2)$ complex was found to spontaneously isomerize in solution to give *mer*-$Mo(CO)_3(dppe)(\eta^1\text{-}SO_2)$. Along with the change in the SO_2 bonding mode upon isomerization, there is a change in the lability of the SO_2 ligand. The η^2-SO_2 ligand in the *fac* complex is readily displaced by excess MeCN in a few hours at 25 °C, but the η^1-planar SO_2 in the *mer* complex shows no sign of reaction after days under these conditions. The tungsten analogues are similar; however, the substitution of CH_3CN by SO_2 in *fac*-$W(CO)_3(dppe)(MeCN)$ proceeds at a rate comparable to the isomerization of the *fac* complex to the *mer* species, and thus we were unable to obtain *fac*-$W(CO)_3(dppe)(\eta^2\text{-}SO_2)$ free of the *mer* η^1-SO_2 complex. The complex *mer*-$Mo(CO)_3(dppe)(\eta^1\text{-}SO_2)$ could also be prepared by photolysis of a solution of $Mo(CO)_4(dppe)$ in the presence of excess SO_2.

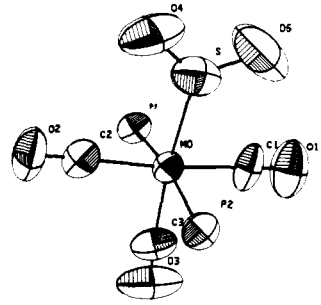

Figure 1. ORTEP projection of $Mo(CO)_3(P\text{-}i\text{-}Pr_3)_2(SO_2)$ (Ia). Isopropyl groups have been omitted for clarity.

Use of the highly basic and bulky phosphines P-*i*-Pr_3 and PCy_3 led to isolation of new SO_2 complexes, *mer,trans*-$Mo(CO)_3(PR_3)_2(SO_2)$, (I Table I). Analogous tungsten complexes were also synthesized, in higher yield (50–80%). In general, the PCy_3 complexes were more stable and more readily prepared than the P-*i*-Pr_3 species. Addition of 2 equiv of less sterically demanding phosphines such as PPh_3 to $Mo(CO)_3(NCMe)_3$ followed by treatment with SO_2 gave intractable products. The X-ray crystal structure of *mer,trans*-$Mo(CO)_3(P\text{-}i\text{-}Pr_3)_2(SO_2)$ was determined and revealed (Figure 1) that (a) the carbonyls had rearranged from facial in $Mo(CO)_3(NCMe)_3$ to the meridional configuration, presumably due to the steric requirements of the bulky phosphines and (b) the MSO_2 coordination geometry was η^1-planar rather than η^2. These features will be discussed in more detail later, but at this point it is clear that the mode of SO_2 bonding is indeed sensitive to ancillary ligand variations.

A second route to Ia–d was devised with the use of *fac*-$M(CO)_3(C_7H_8)$ (C_7H_8 = η^6-cycloheptatriene) as a starting material (eq 2). In this case, both the yields and product purity were found

$$fac\text{-}M(CO)_3(C_7H_8) \xrightarrow[2.\ SO_2]{1.\ 2PR_3} mer,trans\text{-}M(CO)_3(PR_3)_2(SO_2) + C_7H_8 \quad (2)$$

Ia, M = Mo; R = *i*-Pr
Ib, M = Mo; R = Cy
Ic, M = W; R = *i*-Pr
Id, M = W; R = Cy

to be improved for M = Mo. Even more significantly, the reaction under *argon* stopped after the first step yielded novel five-coordinate species $M(CO)_3(PCy_3)_2$ (M = Mo, W), which reversibly add N_2, H_2, or C_2H_4 but irreversibly add SO_2 to give Ib or Id.[10] If the reaction is performed in a nitrogen atmosphere prior to SO_2 addition, the dinitrogen complex *mer,trans*-$M(CO)_3(PCy_3)_2(N_2)$ precipitates initially.[10] However, since the N_2 is reversibly bound, SO_2 will displace it to form the irreversibly bound SO_2 species.

The PPh_3 analogue Ie cannot be prepared from $Mo(CO)_3(C_7H_8)$ but can be obtained from the reaction of *cis,trans*-$Mo(CO)_2(PPh_3)_2(SO_2)(NCMe)$ (vide infra) with CO and, unlike

(18) Cromer, D. T.; Waber, J. T. "International Tables for X-ray Crystallography"; Kynoch Press: Birmingham, England, Table 2.2A; Cromer, D. T., Table 2.3.1.

(19) Kubas, G. J. *Inorg. Chem.* **1979**, *18*, 182.

Table VI. Effect of Ancillary Ligands on SO_2 Coordination Geometry and Infrared Frequencies[a]

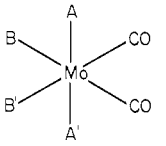

	A	A'	B	B'	ν(SO), cm^{-1}	ν(CO), cm^{-1}	ν(CN), cm^{-1}
η^2-SO_2	SO_2	SO_2	bpy	bpy	1138, 873[b]	2000, 1953[b]	
	SO_2	CO	phen	phen	1149, 935[b]	1984, 1898[b]	
	SO_2	CO	dppe	dppe	(1159, 1150), 927	1984, 1913, 1894	
	SO_2	PPh_3	bpy	bpy	1107, 903[b]	1898, 1805[b]	
	PPh_3	PPh_3	SO_2	MeCN	1138, 910	1920, 1836	*c*
	PPh_3	PPh_3	SO_2	py	1130, 905	1928, 1820	
η^2-SO_2 + η^1-SO_2	PPh_3	PPh_3	SO_2	CN-*t*-Bu	1119, 906 1229, 1066	1937, 1875 1958, 1892	2123
	PPh_3	PPh_3	SO_2	CNCy	1119, 912 1225, 1064	1931, 1872 1956, 1890	2121
η^1-SO_2	PPh_3	PPh_3	SO_2	CN (*p*-tolyl)	1227, 1065	1960, 1876	2108
	PPh_3	PPh_3	SO_2	CO	1254, 1080	2015, 1953, 1908	
	P-*i*-Pr_3	P-*i*-Pr_3	SO_2	CO	1237, 1071	1997, 1931, 1889	
	PCy_3	PCy_3	SO_2	CO	1239, 1070	1996, 1917, 1886	
	SO_2	dppe	dppe	CO	1229, 1071	2031, 1929	
	PPh_3	PPh_3	bpy	bpy		1797, 1727[b]	
	PPh_3	PPh_3	MeCN	MeCN		1814, 1745[d]	
	PPh_3	PPh_3	CN-*t*-Bu	CN-*t*-Bu		1853, 1804	2119, 2075
	PPh_3	PPh_3	CNCy	CNCy		1861, 1811	2128, 2106
	PPh_3	PPh_3	CN (*p*-tolyl)	CN (*p*-tolyl)		1862, 1829	2084, 2040

[a] Nujol mull spectra. [b] Reference 12. [c] Not observed. [d] Reference 7

Ia–Id, is unstable in solution to isomerization and/or disproportionation.

The complexes Ia–Ie do not reversibly lose SO_2 on heating, and although they decompose in solution in the presence of atmospheric oxygen, they do not form sulfato species. This is consistent with the general behavior of complexes containing η^1-planar SO_2.[2,19]

Preparation and Properties of *cis,trans*-$Mo(CO)_2(PPh_3)_2(SO_2)$(L) (II). In order to examine the effect of varying only one ancillary ligand on the metal–SO_2 coordination geometry, a series of complexes (II) was prepared. The synthetic route to II involved

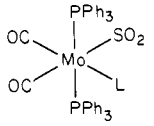

II

passage of excess SO_2 through a MeCN slurry of the known complex, *cis,trans*-$Mo(CO)_2(PPh_3)_2(NCMe)_2$,[7] which gave lavender microcrystals of *cis,trans*-$Mo(CO)_2(PPh_3)_2(\eta^2\text{-}SO_2)$(NCMe) (II, L = NCMe). The MeCN can be readily substituted to give II with a variety of L groups. The Mo–SO_2 coordination geometry of series II is remarkably dependent upon the nature of L, as seen in Table VI and discussed below.

Treatment of II (L = NCMe) with bipyridyl was found to give the known[12] complex $Mo(CO)_2(bpy)(PPh_3)_2$, indicating that the η^2-SO_2 ligand is more readily displaced than either PPh_3 or CO.

Preparation and Reactions of $[Mo(CO)_2(py)(PPh_3)(\mu\text{-}SO_2)]_2$. The following reaction has been found to occur slowly (within ca. 20–60 min) in dichloromethane solution at ambient temperature:

$$2cis,trans\text{-}Mo(CO)_2(PPh_3)_2(py)(\eta^2\text{-}SO_2) \rightarrow [Mo(CO)_2(py)(PPh_3)(\mu\text{-}SO_2)]_2 + 2PPh_3 \quad (3)$$

The structure of the dimer (Figure 2) revealed a novel bridging SO_2 geometry.[4] The basicity of the terminal oxygen of η^2-SO_2 must be relatively high in order for it to effectively displace a PPh_3, especially since dimerization occurs even in the presence of a large excess of PPh_3 or pyridine. This is borne out by the surprisingly high resistance of the dimer to cleavage. For example, prolonged treatment with a large excess of pyridine merely resulted in displacement of the remaining PPh_3 to give $[Mo(CO)_2(py)_2(\mu\text{-}SO_2)]_2$. Decomposition did occur in refluxing pyridine, and overnight reaction with excess $P(OMe)_3$ in CH_2Cl_2 did cleave the dimer, giving $Mo(CO)_2[P(OMe)_3]_3(SO_2)$, but the necessity of such forcing conditions was unexpected. Infrared data (Table II, supplementary material) indicated that the phosphite complex contained η^1 SO_2.[2,19] An attempt to methylate the oxygen atom of the SO_2 in $[Mo(CO)_2(py)(PPh_3)(\mu\text{-}SO_2)]_2$ with $MeSO_3F$ resulted in decomposition to uncharacterized species that exuded the characteristic odor of organosulfur compounds.

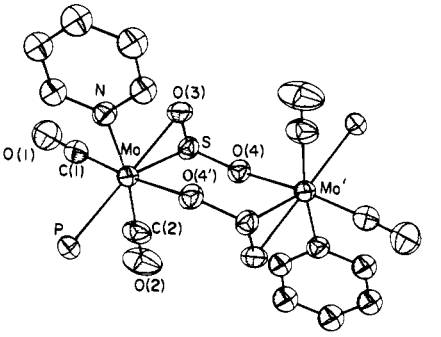

Figure 2. ORTEP projection of $[Mo(CO)_2(py)(PPh_3)(\mu\text{-}SO_2)]_2$ (III). Phenyl rings have been omitted.

A cyclohexylamine analogue, $[Mo(CO)_2(CyNH_2)(PPh_3)(\mu\text{-}SO_2)]_2$, was also prepared and possessed properties similar to the pyridine species.

Infrared and NMR Studies. Johnson and Dew have shown that the η^1-planar complex $[Ru(NH_3)_4Cl(SO_2)]Cl$ can be photolyzed at low temperature in the solid to an η^2 form plus other unidentified products and that the η^1-planar $\rightarrow$ η^2 SO_2 isomerization is reversed by warming. Our studies indicate that the energy difference between η^1 and η^2 SO_2 in II is small since either of the conformations can be stabilized by small changes in the σ- and/or π-bonding characteristics of one ancillary ligand. In fact the complexes with L = alkylisocyanide contain both forms in approximately equal amount in the solid as evidenced by the IR frequencies. Although IR results indicate that the η^1-planar form predominates in solutions (Table II), repeated recrystallization at room temperature did not change the ratio observed in the solid. Attempts were made to study the dynamics of this process in

Table VII. ^{31}P and ^{17}O NMR Data

compound	$\delta(^{31}P)$,[a] ppm	$\delta(^{17}O)$,[b] ppm	^{17}O signal width at half height, Hz
II (L = CNCy)	+44.8	420	800
II (L = CN (*p*-tolyl))	+43.5, 24.3	416	800
$Mo(CO)_3(py)_2(\eta^2\text{-}SO_2)$		234	300
$Mo(CO)_2(PPh_3)_2(CNCy)_2$	+54.3		
$Mo(CO)_2(PPh_3)_2(CN\text{-}t\text{-}Bu)_2$	+54.2		
$Mo(CO)_2(PPh_3)_2[CN(p\text{-tolyl})]_2$	+53.3		

[a] CH_2Cl_2 solutions; reference Me_3PO_4. [b] CH_2Cl_2 solutions of compounds with isotopically enriched SO_2 (33% ^{17}O); reference H_2O. For free SO_2, δ = 512 ppm.

solution by ^{17}O and ^{31}P NMR techniques.

The ^{17}O (33% $S^{17}O_2$) NMR spectra of selected complexes (Table VII) were recorded in CH_2Cl_2 solution at room temperature and at −50 °C. Only one ^{17}O resonance was evident in all of these spectra. The observation of only one peak for *fac*-$Mo(CO)_3(py)_2(\eta^2\text{-}SO_2)$, which is exclusively η^2 in solution by IR measurements, can be attributed to one of two possibilities: rapid interconversion of the two oxygen environments, perhaps through an η^1-planar intermediate, or quadrupolar broadening of the bound oxygen in a static structure. One should notice, however, that there is a large chemical shift difference between those complexes that are predominantly one form in solution, which points to the utility of ^{17}O NMR as a diagnostic.

The ^{31}P NMR spectra of II (L = CNCy and L = CN(*p*-tolyl)) were observed down to −50 °C (Table VII), but again no evidence was found for an interconversion of isomers. In addition to a major resonance near 44 ppm, other weak resonances were observed that are likely due to decomposition and/or isomerization, especially since a significant peak due to free PPh_3 was observed. The room-temperature spectrum of II (L = CNCy) is given as supplementary data (Figure 5).

The IR spectrum of $[Mo(CO)_2(py)(PPh_3)(\mu\text{-}SO_2)]_2$ shows ν(SO) bands at 1043 and 919 cm^{-1}. The position of the low-energy S–O stretch is similar to that for other η^2-SO_2 complexes of Mo (the parent complex II (L = py) shows ν(SO) at 1130 and 905 cm^{-1}), but the high-energy band is at least 60 cm^{-1} below that for other Mo η^2-SO_2 complexes. This provided the first indication that coordination of the terminal oxygen of the η^2 SO_2 was oc-

Table X. Fractional Coordinates and Thermal Parameters for $Mo(CO)_3(P\text{-}i\text{-}Pr_3)_2(SO_2)$[a]

atom	x	y	z	atom	x	y	z
Mo(1)	0.12461 (3)	0.03719 (4)	0.25159 (5)	C(1)	0.1742 (4)	0.1239 (6)	0.1945 (9)
O(1)	0.2028 (3)	0.1719 (6)	0.1676 (7)	C(2)	0.0783 (4)	−0.0578 (6)	0.2999 (8)
O(2)	0.0530 (3)	−0.1118 (4)	0.3272 (6)	C(3)	0.1384 (4)	0.0858 (7)	0.3833 (8)
O(3)	0.1473 (4)	0.1146 (6)	0.4520 (7)	S(1)	0.1099 (1)	−0.0038 (2)	0.0981 (2)
O(4)	0.0745 (4)	−0.0739 (6)	0.0741 (6)	O(5)	0.1335 (4)	0.0434 (7)	0.0175 (7)
P(1)	0.2066 (1)	−0.0551 (2)	0.2815 (2)	C(4)	0.2129 (5)	−0.0983 (8)	0.4045 (9)
C(5)	0.1688 (5)	−0.1126 (9)	0.4627 (9)	C(6)	0.2588 (6)	−0.1654 (9)	0.4152 (10)
C(7)	0.2714 (5)	0.0030 (11)	0.2659 (11)	C(8)	0.3207 (7)	−0.0485 (15)	0.2448 (16)
C(9)	0.2776 (5)	0.0783 (8)	0.3431 (10)	C(10)	0.2184 (4)	−0.1438 (7)	0.2023 (8)
C(11)	0.2261 (6)	0.1200 (9)	0.0988 (10)	C(12)	0.1709 (5)	−0.2050 (7)	0.2100 (11)
P(2)	0.0414 (1)	0.1313 (1)	0.2464 (2)	C(13)	−0.0127 (4)	0.0978 (6)	0.1642 (7)
C(14)	−0.0611 (4)	0.1557 (7)	0.1483 (9)	C(15)	−0.0344 (5)	0.0082 (9)	0.1819 (11)
C(16)	0.0123 (5)	0.1522 (9)	0.3657 (9)	C(17)	−0.0050 (7)	0.0762 (10)	0.4209 (11)
C(18)	−0.0325 (6)	0.2193 (10)	0.3718 (10)	C(19)	0.0538 (5)	0.2414 (7)	0.2051 (12)
C(20)	0.0937 (6)	0.2868 (8)	0.2763 (15)	C(21)	0.0715 (6)	0.2415 (11)	0.0997 (14)

[a] Anisotropic thermal parameters are published as supplementary data (Table VIIIa).

Table XI. Fractional Coordinates and Thermal Parameters for $[Mo(CO)_2(py)(PPh_3)(\mu\text{-}SO_2)]_2 \cdot 2CH_2Cl_2$

atom	x	y	z	b	atom	x	y	z	b
Mo(1)	0.42052 (3)	0.09479 (5)	0.12998 (4)	*a*	C(1)	0.4452 (4)	0.2752 (7)	0.2400 (5)	*a*
O(1)	0.4642 (4)	0.3868 (5)	0.3113 (5)	*a*	C(2)	0.4183 (4)	0.2226 (8)	−0.0119 (6)	*a*
O(2)	0.4206 (4)	0.3023 (6)	−0.0910 (5)	*a*	O(3)	0.5661 (3)	0.0876 (4)	0.1891 (3)	*a*
S(1)	0.5869 (1)	0.2033 (2)	0.0927 (1)	*a*	O(4)	0.6078 (3)	0.1365 (4)	−0.0245 (3)	*a*
N(1)	0.3979 (3)	−0.0528 (5)	0.2934 (4)	*a*	C(3)	0.4228 (4)	−0.1783 (7)	0.2953 (5)	*a*
C(4)	0.4211 (5)	−0.2622 (7)	0.3978 (6)	*a*	C(5)	0.3930 (5)	−0.2115 (8)	0.5048 (6)	*a*
C(6)	0.3683 (5)	−0.0839 (9)	0.5019 (6)	*a*	C(7)	0.3704 (4)	−0.0078 (7)	0.3975 (5)	*a*
P(1)	0.2396 (1)	0.0436 (2)	0.0736 (1)	*a*	C(8)	0.2104 (4)	0.2142 (6)	0.0358 (5)	*a*
C(9)	0.1513 (5)	0.2164 (7)	−0.0726 (6)	*a*	C(10)	0.1368 (6)	0.3521 (9)	−0.1014 (7)	*a*
C(11)	0.1818 (5)	0.4856 (8)	−0.0220 (8)	*a*	C(12)	0.2388 (5)	0.4838 (8)	0.0901 (8)	*a*
C(13)	0.2534 (5)	0.3509 (8)	0.1183 (7)	*a*	C(14)	0.1681 (4)	−0.0348 (6)	0.1957 (5)	*a*
C(15)	0.1172 (5)	0.0398 (8)	0.2528 (6)	*a*	C(16)	0.0648 (7)	−0.0228 (12)	0.3458 (7)	*a*
C(17)	0.0635 (7)	−0.1604 (12)	0.3827 (7)	*a*	C(18)	0.1128 (5)	−0.2400 (9)	0.3255 (7)	*a*
C(19)	0.1646 (5)	−0.1768 (8)	0.2332 (6)	*a*	C(20)	0.1710 (4)	−0.0972 (6)	−0.0642 (5)	*a*
C(21)	0.2149 (4)	−0.1004 (7)	−0.1678 (5)	*a*	C(22)	0.1645 (5)	−0.2054 (8)	−0.2741 (6)	*a*
C(23)	0.0702 (5)	−0.3054 (8)	−0.2761 (7)	*a*	C(24)	0.0264 (5)	−0.3011 (8)	−0.1748 (7)	*a*
C(25)	0.0754 (4)	−0.1987 (7)	−0.0697 (6)	*a*	C(26)	0.2964 (10)	0.3751 (13)	0.6113 (18)	*a*
Cl(1)	0.2569 (4)	0.1977 (5)	0.6128 (4)	*a*	Cl(2)	0.1954 (3)	0.4357 (4)	0.5349 (6)	*a*
H(1)	0.4374 (47)	−0.2075 (72)	0.2304 (59)	5.0 (0)	H(2)	0.4374 (47)	−0.3443 (72)	0.3900 (58)	5.0 (0)
H(3)	0.3917 (44)	−0.2652 (68)	0.5796 (59)	5.0 (0)	H(4)	0.3600 (53)	−0.0421 (80)	0.5506 (63)	5.0 (0)
H(5)	0.3537 (45)	0.0750 (72)	0.4043 (58)	5.0 (0)	H(6)	0.1250 (46)	0.1280 (71)	−0.1281 (57)	5.0 (0)
H(7)	0.1149 (47)	0.3479 (71)	−0.1806 (59)	5.0 (0)	H(8)	0.1726 (43)	0.5887 (70)	−0.0301 (54)	5.0 (0)
H(9)	0.2716 (44)	0.5860 (72)	0.1351 (56)	5.0 (0)	H(10)	0.2712 (49)	0.3384 (75)	0.1905 (59)	5.0 (0)
H(11)	0.1175 (46)	0.1282 (73)	0.2210 (59)	5.0 (0)	H(12)	0.0286 (47)	0.0151 (71)	0.3876 (59)	5.0 (0)
H(13)	0.0263 (46)	−0.2071 (69)	0.4451 (59)	5.0 (0)	H(14)	0.1189 (45)	−0.3388 (74)	0.3325 (59)	5.0 (0)
H(15)	0.1963 (48)	−0.2248 (74)	0.2021 (60)	5.0 (0)	H(16)	0.2833 (47)	−0.0301 (69)	−0.1684 (56)	5.0 (0)
H(17)	0.1887 (48)	−0.2130 (74)	−0.3369 (59)	5.0 (0)	H(18)	0.0466 (47)	−0.3801 (72)	−0.3394 (60)	5.0 (0)
H(19)	−0.0251 (48)	−0.3532 (76)	−0.1766 (64)	5.0 (0)	H(20)	0.0420 (45)	−0.1978 (67)	0.0001 (58)	5.0 (0)

[a] Anisotropic thermal parameters are published as supplementary data (Table IXa).

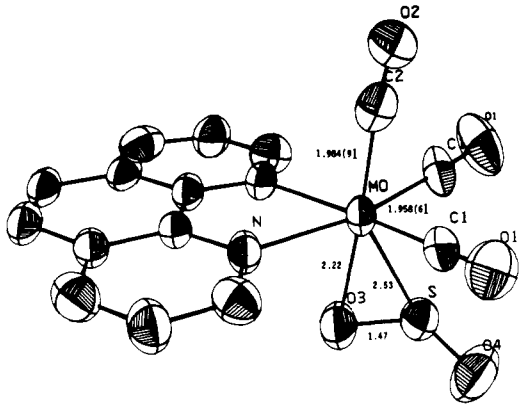

Figure 3. ORTEP projection of $Mo(CO)_3(phen)(\eta^2\text{-}SO_2)$ (from ref 1).

curring and led us to undertake a single-crystal X-ray diffraction study of the dimer.

Lastly, Table II lists observed ν(SO) for Nujol mulls of the isotopically labeled complexes used for ^{17}O NMR studies. The isotopic shifts, which can be cleanly resolved into the expected three components due to $S^{17}O^{17}O$, $S^{17}O^{18}O$, and $S^{18}O^{18}O$ for each SO stretching mode in *fac*-$Mo(CO)_3(py)_2(\eta^2\text{-}SO_2)$, confirm that the bands are properly assigned. The CO frequencies showed no observable shifts (± 1 cm^{-1}) compared to the unlabeled complexes.

Discussion

Bonding Concepts. Consideration of the MO template of a five-coordinate fragment of a d^6 octahedral complex indicates that SO_2 can bind to the metal in the η^1-planar or η^2 geometries but not in the η^1-pyramidal form.[2] In the molecular orbital picture for the η^1-planar structure, the $4a_1$ HOMO of SO_2 donates an electron pair into the vacant σ orbital of the octahedral fragment and the empty $2b_1$ LUMO of SO_2 accepts electron density from the filled π-backbonding orbitals. When SO_2 binds in the η^2 form, the dominant interaction is attributed to donation from the metal π orbitals into the $2b_1$ orbital, which is oriented to accept electron density through both the sulfur and oxygen lobes of the $2b_1$, somewhat resembling the coordination of an unsymmetrical olefin. The octahedral fragment lacks a filled σ-donor-type orbital needed for η^1-pyramidal coordination of the SO_2. All the reported structures of d^6 complexes containing SO_2 indeed show η^1-planar or η^2 geometries for the SO_2 ligand.[2]

Assuming this simple picture accounts for the difference in the η^1-planar and η^2 coordination modes, properties of the octahedral fragment that tend to favor one type of SO_2 coordination over another have been discussed.[2] The η^2 geometry involves more M $\rightarrow$ SO_2 π donation and less SO_2 $\rightarrow$ M σ donation than does the η^1-planar case. Thus, the tendency toward the η^2 geometry would be favored by factors such as increased metal basicity and ancillary ligands which are strong σ donors and/or poor π acceptors since such changes would increase the energy of the σ-accepting orbital or enhance the π basicity of the complex fragment.

Another factor that may have considerable influence on the coordination geometry of SO_2 is illustrated by the molecular structures of the two d^6 η^2-SO_2 complexes that have been characterized by X-ray diffraction (Figures 3 and 4).[1] In both complexes the coordinated S–O bonds are oriented so that the sulfur atom lies closest to CO ligands. This has been attributed to a polarization of π-electron density toward the better π-accepting ligands (CO > bpy or phen) in the plane cis to the SO_2.[2] The unsymmetrical η^2-SO_2 ligand is oriented to best compete for the π-electron density with the sulfur atom nearer the carbonyls since the $2b_1$ acceptor orbital is largely sulfur p_z in character with a smaller oxygen p_z contribution. This orientation of the S–O bond with the S atom nearer the better π-acceptor ligand (where a disparity exists) has been observed in all the structures of η^2-SO_2 complexes reported to date.[2] This suggests that the presence of a considerable difference in the π-acceptor abilities of ligands cis to the coordinated SO_2 would favor the η^2 geometry over η^1-planar.

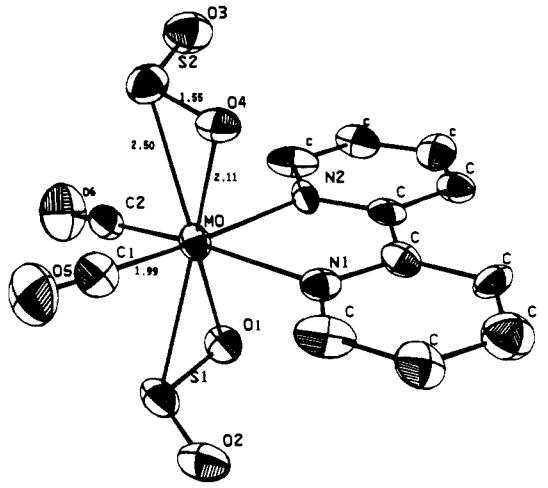

Figure 4. ORTEP projection of $Mo(CO)_2(bpy)(\eta^2\text{-}SO_2)_2$ (from ref 1).

$Mo(CO)_2(PPh_3)_2(SO_2)L$ Complexes. The new SO_2 complexes reported here fit very well into this bonding model for SO_2 coordination. A graphic illustration of this is provided by the complexes II, where changing one ligand in the complex can alter the SO_2 coordination to give η^1-planar SO_2, η^2-SO_2, or a mixture of both forms (Table VI). The ν(CO) frequencies of a series of compounds closely related to II, *cis,trans*-$Mo(CO)_2(PPh_3)_2L_2$, is shown in Table VI. These ν(CO) frequencies provide a measure of the π back donation into the CO π^* orbitals. In order of increasing π density found on the metal, the series is CO < CN(*p*-tolyl) < CNCy < CN-*t*-Bu < NCMe < bpy. Thus, it is apparent from the complexes II that the η^2-SO_2 correlates with the better σ-donor ligands and the η^1-planar SO_2 with the stronger π acceptors. The substitution of a poorer π acceptor for a CO cis to the SO_2 in changing from II (L = CO) to II (L = py) also induces an asymmetry in the π donor orbitals, which could promote the η^2 geometry.

Remarkably, the alkylisocyanide complexes II (L = CN-*t*-Bu or CNCy) display two sets of ν(SO) and ν(CO) of about equal intensity in the mull spectrum of the solid that indicate the presence of both η^2 and η^1-planar SO_2. The isocyanides are excellent σ donors and good π acceptors, and for the *tert*-butyl and cyclohexyl isocyanides, the electronic situation in the complex has apparently reached a point where the η^2 and η^1-planar SO_2 coordination modes are quite close energetically. Merely changing the isocyanide R group from alkyl to aryl eliminates any infrared indication of the η^2 geometry.

Only one case of linkage isomerism in transition-metal SO_2 complexes has previously been reported, and that involved photolysis of $[RuCl(NH_3)_4(\eta^1\text{-}SO_2)]Cl$ in the solid state at low temperature to give an apparently η^2-SO_2 form as well as other as yet unidentified species.[20] The molybdenum compounds are unique in that the isomers form spontaneously and are stable in solution, in which the η^1-planar form predominates. At this point the ^{17}O and ^{31}P NMR spectra have not yielded any definitive dynamical information, but the possibly fluxional nature of the η^2-SO_2 bond is being examined further.

$M(CO)_3P_2(SO_2)$ Complexes. The complexes Ia–e contain SO_2 coordinated in the η^1-planar mode as indicated by the ν(SO) frequencies and verified by a crystal structure for Ia (Figure 1). The structure also confirms the stereochemistry of Ia–e assigned from spectroscopic data with mutually trans phosphines and a meridional arrangement of the three CO ligands (the complex Ie is identical with II (L = CO) and is in fact best prepared from II (L = CH_3CN) by addition of CO). The Mo–S distance in Ia of 2.285 (3) Å is the longest such distance for the η^1-planar geometry recorded to date. Indeed this distance is longer than the 2.239 (3) Å exhibited by $OsHCl(CO)(PCy_3)_2(SO_2)$,[21] which shows an unusual (for η^1-planar complexes) lability of the SO_2

(20) Johnson, D. A.; Dew, V. C. *Inorg. Chem.* **1979**, *18*, 3273.
(21) Ryan, R. R.; Kubas, G. J. *Inorg. Chem.* **1978**, *17*, 637.

ligand and an unusual reactivity with O_2 to readily form the sulfato complex $OsCl(CO)(PCy_3)_2(SO_4)$. In spite of the long Mo–S distance, the SO_2 ligand of Ia does not show these unusual properties. However, the Os–P and Os–CO distances of 2.42 and 1.93 Å, respectively, when compared to the corresponding Mo–P and Mo–CO distances in Ia, indicate that a correction of ca. –0.1 Å should be applied to the Mo–S distance for the purpose of comparing bond strengths. Thus, the structural data is not inconsistent with a stronger M–SO_2 bond in Ia relative to the Os complex.

Some other features of the SO_2 bonding in Ia and $OsHCl(CO)(PCy_3)_2(SO_2)$ are worthy of note. The unusual lability of the SO_2 in the Os complex has been attributed to the strong trans influence of the hydride ligand, which weakens the Os–S bond.[21] The presence of such a strong σ-donor ligand trans to the SO_2 and of a donor–metal–π-acceptor arrangement of ligands cis to the SO_2 (the chloride is trans to the CO) would seem to favor the η^2 geometry over the η^1-planar in the Os complex on the basis of the bonding model discussed above. However, the lower overall π basicity of the Os(II) center relative to Mo(0) favors the η^1-planar geometry and presumably this factor dominates in the Os complex. The rotational orientation of the η^1-planar SO_2 ligand in Ia is such that the SO_2 plane is perpendicular to the plane containing the sulfur, phosphorus, and metal atoms, which is also the orientation in the Os complex. Thus the $2b_1$ acceptor orbital of the SO_2 is aligned for π backbonding in both complexes so as to minimize competition with the CO ligands for π-electron density.

The stereochemistry of the octahedral complex can also influence the SO_2 coordination mode as demonstrated by the geometrical isomers *fac*-$Mo(CO)_3(dppe)(\eta^2\text{-}SO_2)$ and *mer*-$Mo(CO)_3(dppe)(\eta^1\text{-}SO_2)$. The η^2-SO_2 complex is a phosphine analogue of the phenanthroline complex *fac*-$Mo(CO)_3(phen)(\eta^2\text{-}SO_2)$ and presumably has a similar structure (see Figure 3). In solution the *fac* complex rearranges to give the *mer* isomer in which the SO_2 adopts an η^1-planar geometry as indicated by the $\nu(SO)$ frequencies. The driving force for the isomerization might be due to a net stabilization resulting from a reduced competition between the three CO ligands and the SO_2 for π-electron density (the dppe ligand is a relatively poor π acceptor). In the *fac* complex, all three carbonyls compete with the η^2 SO_2 (as well as with each other) for d π electrons. However, in the *mer* isomer, the SO_2 ligand (η^1-planar or η^2) can be oriented to place the $2b_1$ acceptor orbital in the plane containing the CO, the metal, and phosphorus atoms so that only one CO is competing with the SO_2 for d π electrons. Obviously, the energy difference between η^1-planar and η^2-SO_2 coordination can be small in these octahedral Mo complexes, hence subtle factors may influence the form chosen. This would appear to be the case in the change of SO_2 coordination geometry that occurs during the *fac* to *mer* isomerization. One factor that would favor the η^1-planar geometry in the *mer* complex is the decrease in polarization of π-electron density in the plane cis to the SO_2 relative to the *fac* isomer since there exists only one assymmetric plane in the *mer* complex.

As in series I, the coordinated SO_2 in the complexes of series II is neither reversibly bound nor reactive with oxygen to form sulfato complexes. For those complexes containing η^1-planar SO_2, this behavior is consistent with the majority of known η^1-planar SO_2 complexes of all metal coordination types.[2] The behavior of the η^2 complexes II, however, is in contrast to that of η^2-SO_2 in four- and five-coordinate complexes.[2] One important difference between the octahedral η^2-SO_2 complexes and the lower coordinate systems is the inaccessibility of the η^1-pyramidal SO_2 bonding mode in the octahedral complexes noted above in the discussion of the SO_2 bonding model. In general, the η^1-pyramidal SO_2 geometry is not far removed energetically for the four- and five-coordinate η^2-SO_2 complexes. The great majority of η^1-pyramidal SO_2 complexes contain reversibly bound SO_2 and react with oxygen to give sulfato complexes.[2] Thus, an intermediate species containing an η^1-pyramidal SO_2 might be involved in the reversible coordination of SO_2 and sulfato reaction of the four- and five-coordinate η^2-SO_2 complexes. For the octahedral η^2-SO_2 systems, such a reaction pathway would be blocked by the very high energy of the η^1-pyramidal species.

$[Mo(CO)_2(py)(PPh_3)(\mu\text{-}SO_2)]_2$. Depending upon L, solutions of II show varying degrees of instability toward isomerization or changes in composition. In particular, II (L = py), which contains an η^2-SO_2 ligand, has been found to dissociate PPh_3 in CH_2Cl_2 solution and dimerize to yield crystals of $[Mo(CO)_2(py)(PPh_3)(\mu\text{-}SO_2)]_2 \cdot 2CH_2Cl_2$. This complex features a new type of SO_2 bridging geometry in which all three atoms of SO_2 are metal coordinated.[4]

The structure of the dimer (Figure 2) indicates that rearrangement of the coordination geometry about the metal occurs in addition to phosphine dissociation during formation of the dimer from II (L = py). The coordinated S–O bond is trans to a carbonyl in II (L = py) but is trans to PPh_3 in the dimer. As described in the Experimental Section, a new species that is apparently an isomer of II (L = py) can be isolated from solutions of this complex before extensive formation of the dimer occurs. The infrared spectrum of the new species indicates it contains mutually cis CO ligands, which implies the PPh_3 groups must be mutually cis. Three geometrical isomers of II (L = py) are possible with mutually cis carbonyls and phosphines. Two of the three geometrical isomers would have the three strong π-acceptor ligands trans to the three good σ-donor ligands. Thus the driving force for the isomerization could be a stabilization due to minimizing competition between the strong π acceptors CO and SO_2. In one of these two isomers, loss of a phosphine cis to the SO_2 could lead directly to the observed dimer. A mutually cis arrangement of the bulky phosphine ligands would increase the tendency to dissociate PPh_3, promoting the assembly of the dimer.[22]

The structure of the dimer also shows that the sulfur atom of the η^2-coordinated S–O bond is closer to the better π acceptor (CO) along the N–Mo–C(2) axis. The Mo–C(2) bond distance (1.994 (10) Å) is dramatically longer than the Mo–C(1) distance (1.894 (9) Å). This lengthening of the Mo–C(2) bond can be attributed primarily to the competition between CO(2) and the η^2 SO_2 for π electrons (see also ref 1).

The formation of the dimer from II (L = py) is one of two established examples of coordination of a Lewis acid to the terminal oxygen of an η^2-SO_2 ligand.[3] Our initial attempts to exploit this basicity in reactions of some Mo and W η^2-SO_2 complexes with Lewis acids (as described in the Experimental Section) have yielded little information on the reactivity of the η^2-SO_2 ligand. For example, with *fac*-$Mo(CO)_3(dppe)(\eta^2\text{-}SO_2)$ in CH_2Cl_2 solution, addition of stoichiometric quantities of HCl or BF_3 or rapid stirring with excess HBF_4 results in conversion to *mer*-$Mo(CO)_3(dppe)(\eta^1\text{-}SO_2)$ in minutes whereas the uncatalyzed reaction takes days.[23] This Lewis acid catalysis of an isomerization is apparently not specific to the SO_2 complex as addition of HCl to a solution of *fac*-$Mo(CO)_3(dppe)(PPh_3)$ accelerates conversion to *mer*-$Mo(CO)_3(dppe)(PPh_3)$. The stereochemical consequences of protonation–deprotonation reactions of related octahedral Mo systems of the type $Mo(CO)_2(bipy)_2$ have been studied by Wreford and co-workers.[24] Complexes similar to the cationic seven-coordinate hydrides observed in their work may be important intermediates in the acid-catalyzed rearrangements we observed, but how BF_3 would act to promote these rearrangements is unclear.

Acknowledgment. This work was performed under the auspices of the U.S. Department of Energy, Division of Chemical Sciences, Office of Basic Energy Sciences. We express gratitude to Dr. David C. Moody for preparing isotopically labeled SO_2 and to Dr. Lee J. Todd of Indiana University for the ^{17}O NMR measurements. Also, we acknowledge the Colorado State University Regional NMR Center (supported by National Science Foun-

(22) Cotton, F. A.; Darensbourg, D. J.; Simonetta, K.; Kolthammer, B. W. S. *Inorg. Chem.* **1982**, *21*, 294.

(23) These results, as well as preparation of the $M(CO)_3(dppe)(SO_2)$ derivatives, were confirmed in an independent study reported after submission of this manuscript: Schenk, W. A.; Baumann, F. *Chem. Ber.* **1982**, *115*, 2615.

(24) (a) Datta, S.; Dezube, B.; Kouba, J. K.; Wreford, S. S. *J. Am. Chem. Soc.* **1978**, *100*, 4404. (b) Datta, S.; McNeese, T. J.; Wreford, S. S. *Inorg. Chem.* **1977**, *16*, 2661.

dation Grant No. CHE78-18581) and James S. Frye for recording the ^{31}P NMR spectra.

Registry No. Ia, 84500-95-8; Ib, 73682-36-7; Ic, 84520-53-6; Id, 73682-35-6; Ie, 84500-96-9; II (L = NCMe), 84500-97-0; II (L = CNBu-*t*), 84500-98-1; II (L = py), 84580-17-6; II (L = CNCy), 84537-04-2; III, 84580-18-7; $[Mo(CO)_2(CyNH_2)(PPh_3)(\mu\text{-}SO_2)]_2$, 84500-99-2; $[Mo(CO)_2(py)_2(\mu\text{-}SO_2)]_2$, 84501-00-8; $Mo(CO)_2[P(OMe)_3]_3(SO_2)$, 84501-01-9; $Mo(CO)_2(bpy)(PPh_3)_2$, 15653-24-4; *cis,trans*-$Mo(CO)_2(PPh_3)_2(CNCy)_2$, 84501-02-0; *cis,trans*-$Mo(CO)_2(PPh_3)_2(CNBu\text{-}t)_2$, 84501-03-1; *cis,trans*-$Mo(CO)_2(PPh_3)_2(CNR)_2$ (R = *p*-tolyl), 84501-04-2; *fac*-$Mo(CO)_3(dppe)(\eta^2\text{-}SO_2)$, 84580-19-8; *mer*-$Mo(CO)_3(dppe)(\eta^1\text{-}SO_2)$, 82630-14-6; *fac*-$W(CO)_3(dppe)(\eta^2\text{-}SO_2)$, 82630-10-2; *mer*-$W(CO)_3(dppe)(\eta^1\text{-}SO_2)$, 82630-13-5; *fac*-$Mo(CO)_3(phen)(\eta^2\text{-}SO_2)$, 84580-20-1; *fac*-$Mo(CO)_3(bpy)(\eta^2\text{-}SO_2)$, 84501-05-3; *fac*-$Mo(CO)_3(py)_2(\eta^2\text{-}SO_2)$, 84501-06-4; *fac*-$W(CO)_3(py)_2(\eta^2\text{-}SO_2)$, 84501-07-5; $Mo(CO)_3(C_7H_8)$, 12125-77-8; $Mo(CO)_3(NCMe)_3$, 15038-48-9; $W(CO)_3(C_7H_8)$, 12128-81-3; $W(CO)_3(NCEt)_3$, 84580-21-2; *cis,trans*-$Mo(CO)_2(PPh_3)_2(SO_2)(NCMe)$, 84501-08-6; *cis,trans*-$Mo(CO)_2(PPh_3)_2(NCMe)_2$, 23526-71-8; $Mo(CO)_4(dppe)$, 15444-66-3; *fac*-$W(CO)_3(dppe)(NCMe)$, 84501-09-7; $Mo(CO)_6$, 13939-06-5; $W(CO)_3(NCMe)_3$, 16800-47-8.

Supplementary Material Available: Analytical data (Table I), CO and SO infrared frequencies (Nujol mull and solution data) for complexes not listed in Table VI (Table II), observed and calculated structure factors for $Mo(CO)_3(P\text{-}i\text{-}Pr_3)_2(SO_2)$ and $[Mo(CO)_2(py)(PPh_3)(SO_2)]_2$ (Tables Xb and XIb), and a room-temperature ^{31}P NMR spectrum of II (L = CNCy) in CH_2Cl_2 (Figure 5) (30 pages). Ordering information is given on any current masthead page.

Active Site of Allantoic Purple Acid Phosphatase and a Model Complex for Strongly Coupled Diiron Sites

Garry M. Mockler, John de Jersey, Burt Zerner, Charles J. O'Connor, and Ekk Sinn*

Contribution from the Department of Chemistry, University of Wollongong, NSW, Australia, the Department of Biochemistry, University of Queensland, St. Lucia, Australia 4067, and the Departments of Chemistry, University of New Orleans, New Orleans, Louisiana 70122, and the University of Virginia, Charlottesville, Virginia 22901. *Received August 18, 1982*

Abstract: Magnetic susceptibility determination is able to make powerful structural predictions for the porcine allantoic purple acid phosphatase which is shown to be a diiron enzyme and for the model complexes of type $[Fe(cbpN)]_2O$, which have the same magnetic properties. The presence of the diiron active site in the purple (oxidized) form of the phosphatase is shown by the very low magnetic susceptibility, which can only be attributed to very strong magnetic coupling between two Fe(III) species, and given the absence of any other plausible bridging group, the site can be assigned as Fe–O–Fe. The model complex $[Fe(cbpN)]_2O$ is shown to have this specific site by X-ray crystallography. This complex is also the first example of a central Fe–O–Fe linkage which can be reversed by heating in vacuo or by dissolving in dimethylacetamide. The reduced stability of the Fe–O–Fe linkage is presumably due to the steric strain enforced by the bulky cbpN ligands.

The efficacy of magnetic susceptibility measurements for structure elucidation is sometimes underestimated. With an ultrahigh sensitivity superconducting magnetometer, it is possible to make accurate measurements on quite small samples, or substances, like enzymes, which contain a small unpaired spin density.[1,2]

We are attracted by the controversial nature of the description of the central prosthetic group of purple acid phosphatase, "progesterone induced glycoprotein" (PIG)[3,4] obtained from porcine allantoic fluid (and the very similar protein from beef spleen[5]), which had been suggested to contain either one or two iron sites,[3,4] the known diiron protein hemerythrin,[6] the diiron (sulfur-bridged) protein ferreascid,[7] and model compounds designed to simulate the magnetic properties of these materials.

The enzyme PIG, reputed to have either one or two central iron atoms per molecular weight unit, is an ideal subject for high-precision magnetic susceptibility, since one can expect to distinguish reliably between the magnetic contributions of one and two iron atoms better than with most other physical techniques to which the substance is accessible. The results however produced a surprise. The observed magnetic moment was small ($\lesssim 1.0\ \mu_B$ for one sample and $1.1\ \mu_B$ for another) and constant (4–50 K) within experimental error, less than for even one iron site[8] in the oxidized (purple) form of the protein.[9] This can only reasonably be explained in terms of antiferromagnetic interactions between pairs of iron atoms. In fact, the magnetic moment is so low, that even coupling between two Fe sites of unequal oxidation states is ruled out, for in that case residual electron spin is required. For example, Fe(II) coupled with Fe(III) would leave one unpaired electron, whereas our measurement indicates less than a third of an electron per pair of iron atoms, particularly when spin–orbit coupling is taken into account. Of the possible kinds of equivalent interacting species, Fe(II) is chemically unlikely in the oxidized form, Fe(IV) is quite rare and therefore just as unlikely, so that a pair of Fe(III) sites remains as the plausible species. The possible

*Address correspondence to this author at the University of Virginia.

(1) O'Connor, C. J.; Sinn, E.; Cukauskas, E. J.; Deaver, B. S., Jr. *Inorg. Chim. Acta* **1979**, *32*, 29.
(2) O'Connor, C. J.; Deaver, B. S., Jr.; Sinn, E. *J. Chem. Phys.* **1979**, *70*, 5161.
(3) Campbell, H. D.; Dionysius, D. A.; Keough, T.; Wilson, B. E.; de Jersey, J.; Zerner, B. *Biochem. Biophys. Res. Commun.* **1978**, *82*, 615.
(4) Antanaifis, B. C.; Aisen, P.; Lilienthal, H. R.; Roberts, R. M.; Bazer, F. W. *J. Biol. Chem.* **1980**, *255*, 11204.
(5) Davis, J. C.; Lin, S.; Averill, B. A. *Biochemistry* **1981**, *20*, 4062.
(6) Stenkamp, R. E.; Sieker, L. C.; Jensen, L. H., paper to be presented at San Diego A.C.A. meeting, August 1982.
(7) Hawkins, C. J.; Clark, R. E.; Brewer, G. A.; Sinn, E., unpublished work.
(8) Sinn, E.; O'Connor, C. J.; de Jersey, J.; Zerner, B. "Abstracts of Papers", 183rd National Meeting of the American Chemical Society, Las Vegas, NV, April 1982; American Chemical Society: Washington, DC, 1982; INOR 79. "Abstracts of Papers", 179th National Meeting of the American Chemical Society, Houston, TX, April 1980; American Chemical Society: Washington, DC, 1980; INOR 25.
(9) (a) Details of preparation and purification will be given elsewhere: Sinn, E.; O'Connor, C. J.; de Jersey, J.; Zerner, B. *Inorg. Chim. Acta, Biochem. Sect.*, in press. (b) On treatment with dithionite at pH 4.9., 50% of the iron content is removed rapidly, while the remainder is lost slowly, which also bespeaks a pair of Fe atoms.

0002-7863/83/1505-1891$01.50/0